

## Chapter 4 Measurement

The optical spot scanning system in the thesis contains two main parts, the comb actuator and the photo detector. In this chapter, the characterization of the comb actuator and the optical spot size measured by the reflection type device fabricated by MUMPs are discussed. The preliminary results of the photo detector in the absorption type device are presented.

### 4-1 Comb actuator

The experimental setup used for the comb actuator characterization is shown in Fig 4-1. The resonance frequency and the lateral displacement can be determined from the images taken from the camera. A simple measurement requires only a function generator, a power amplifier and an optical microscope with a digital camera.

An oscillating electrostatic force on the actuator is generated by placing a dc ( $V_{DC}$ ) and an ac ( $V_{AC}$ ) voltage sources in series across the fixed and movable electrodes of the comb actuator. In the measurement,  $V_{DC}$  ranged from 20V to 80 V with the ac peak-to-peak voltage  $V_{AC}$  twice of  $V_{DC}$  (40V to 160V). Resonance is observed under the microscope as the oscillating frequency is scanned across the resonance frequency. The measured resonance frequency was 17.53 KHz in the device with 4 $\mu$ m spring design at  $V_{DC} = 40V$  and  $V_{AC} = 80V$ .

The displacement is measured by comparing the range of oscillation to a known length in the device. For example, the width of the bottom of the triangular reflective mirror is 57.4 $\mu$ m from a WYKO interferometer measurement, as shown in Fig 4-2. The microscope image of resonance of device at  $V_{DC} = 80V$  and  $V_{AC} = 160V$  is

shown in Fig 4-3. The resonance displacement can be determined to be  $20\mu\text{m}$ . Similarly, displacements for various applied voltages can be measured and are listed in Table 4-1.

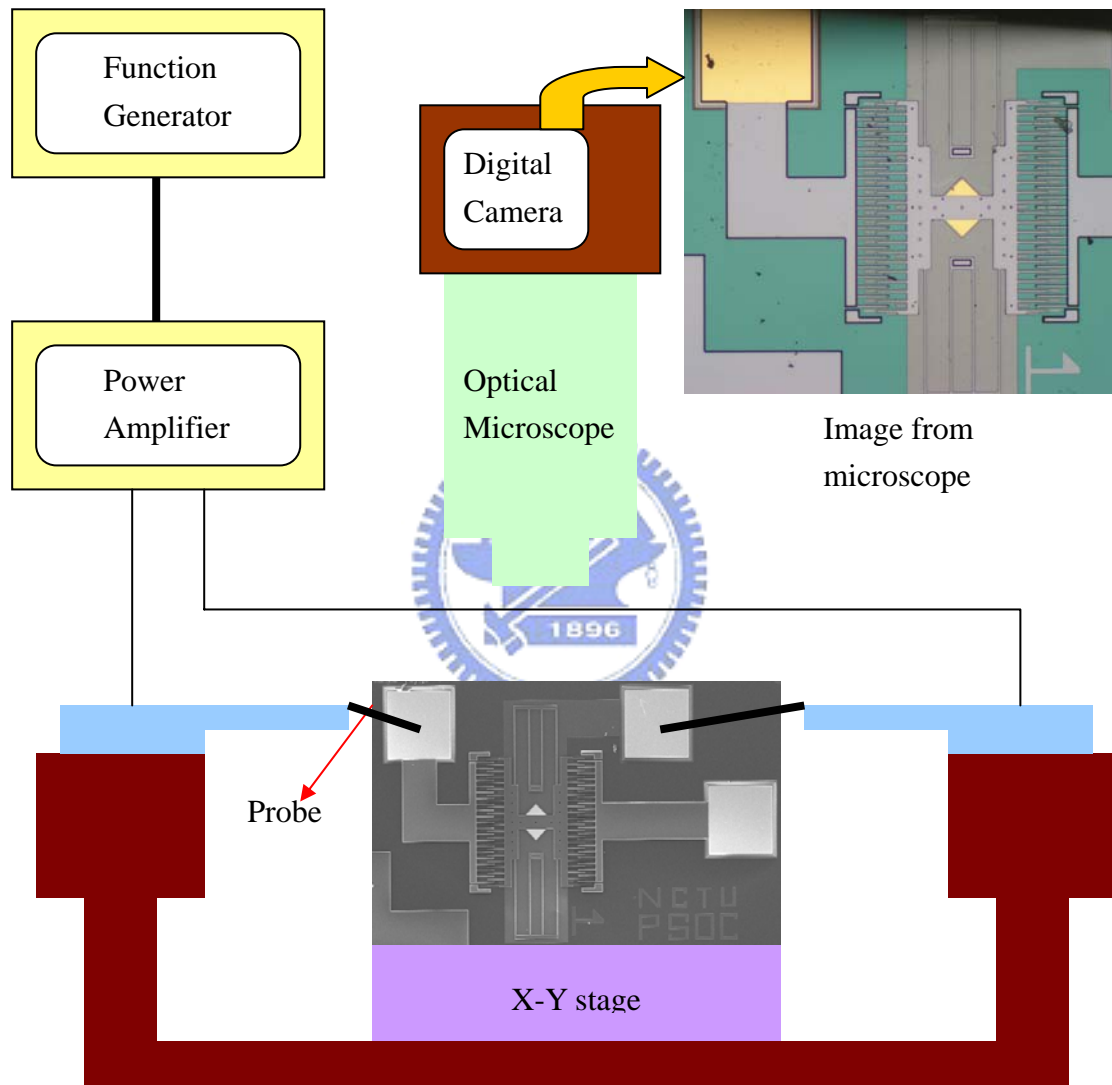
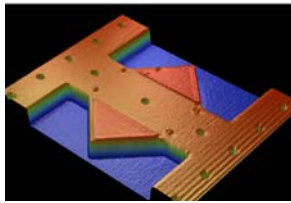
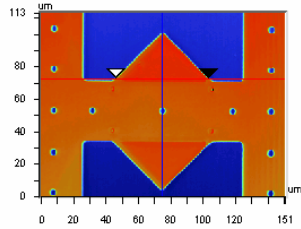


Fig 4-1 Experimental setup for resonance frequency measurement



Title:  
Note:

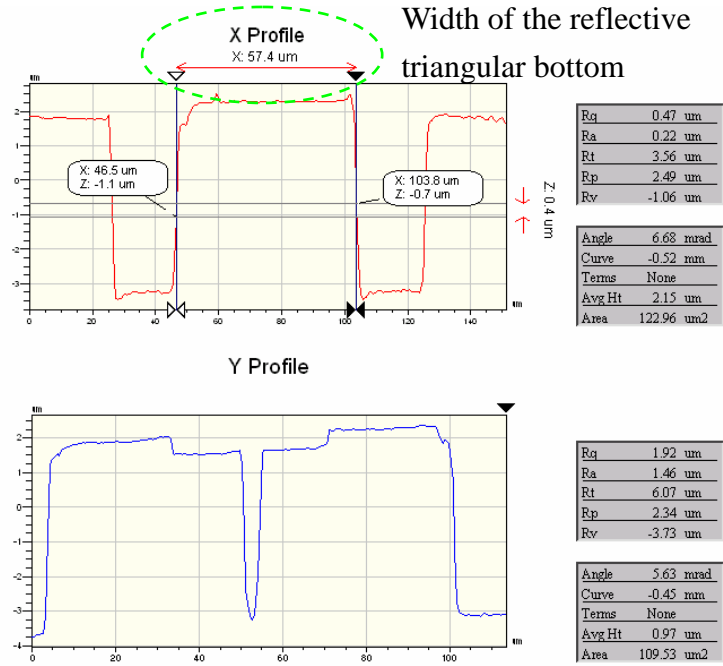


Fig 4-2 WYKO interferometer measurement of the width of the bottom of triangular reflective mirror

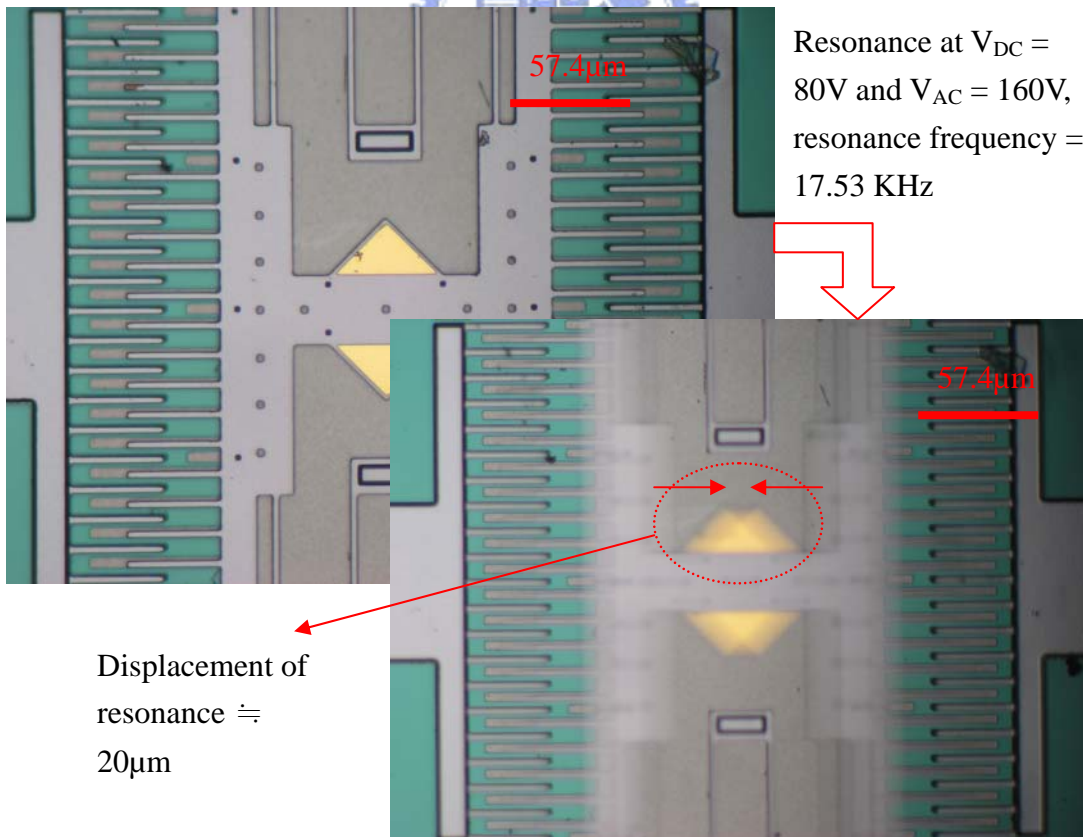
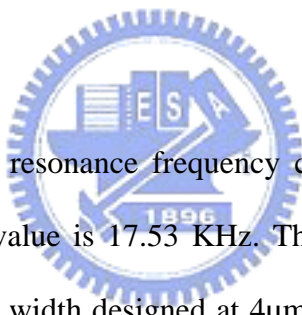


Fig 4-3 Microscope image of the resonance of the device

Applied voltage (V)		Displacement at resonance frequency = 17.53 KHz ( $\mu\text{m}$ )
$V_{\text{DC}}$	$V_{\text{AC}}$	
40	80	8.1
50	100	11.9
60	120	16.1
70	140	18.5
80	160	20

Table 4-1 Measured displacement at resonance



Note that the simulation resonance frequency calculated in Chapter 2 is 26.7 KHz, whereas the measured value is 17.53 KHz. The resonance frequencies of the other four devices with spring width designed at  $4\mu\text{m}$  in the same MUMPs run were also measured to  $17 \pm 1$  KHz. The most important reason might be the loss of the spring width. From Eq 2-7, the resonance frequency is proportional to  $\sqrt{K/m}$ ; from Eq 2-2 the spring constant  $K$  is proportional to the cube of the spring width  $b_s^3$ . If the loss of proof mass  $m$  is negligible, the resonance frequency is proportional to  $\sqrt{b_s^3}$ . From the SEM (Fig 4-4) and WYKO (Fig 4-5) measurements, the spring width is about  $3.1\mu\text{m}$ , 77.5% of the design value in layout. Therefore, the actual frequency should be about  $(77.5\%)^{3/2} = 68\%$  of the calculated value which becomes 18 KHz and is closed to the measured value.

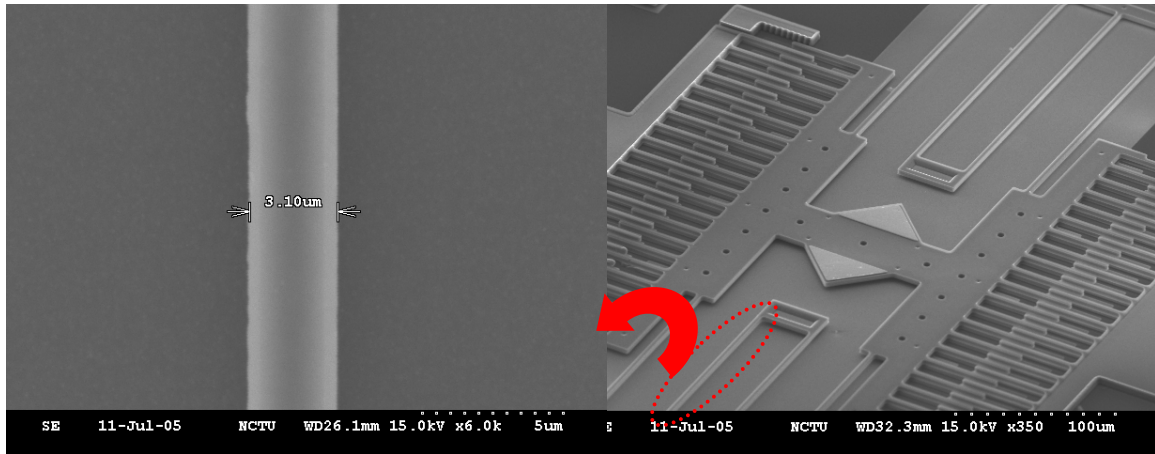


Fig 4-4 Spring width by SEM measurement

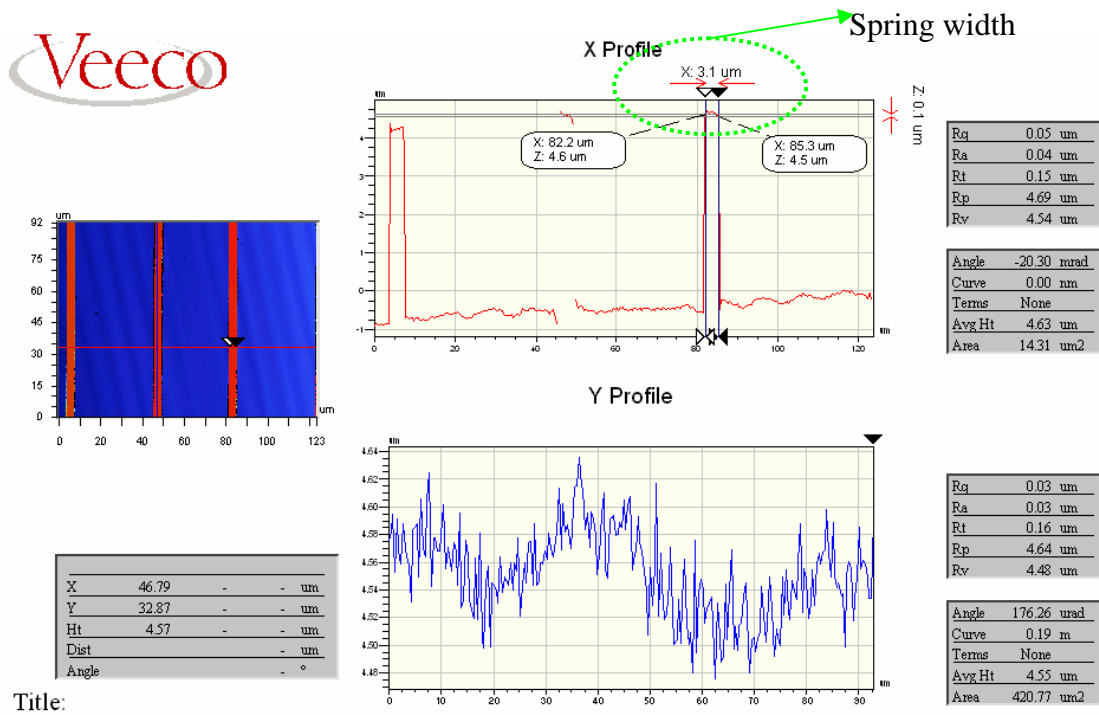


Fig 4-5 Spring width by WYKO measurement

In the device with a layout spring width of  $2\mu\text{m}$ , the calculated resonance frequency is 14.6 KHz. The microscope image of the  $2\mu\text{m}$  device is shown in Fig 4-6(a). Fig 4-6(b) shows the device at resonance with the  $V_{DC} = 20\text{V}$  and  $V_{AC} = 40\text{V}$ . The measured resonance frequency of the device is 4.15 KHz and the spring width measured in WYKO is about  $1\mu\text{m}$ , as shown in Fig 4-7. From the previous discussion, the actual resonance frequency is corrected to be  $(50\%)^{3/2} = 35\%$  of 14.6 KHz, which becomes 5.1 KHz.

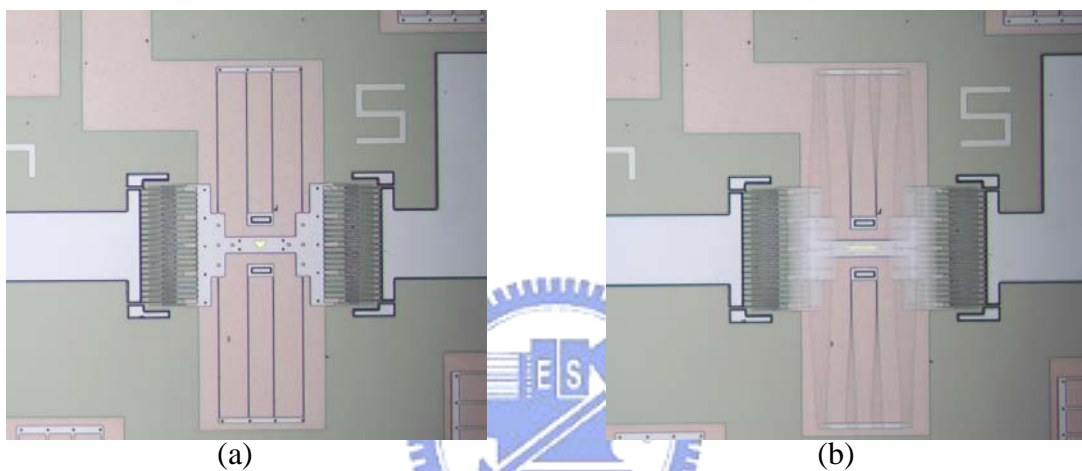


Fig 4-6 (a) Microscope image of the  $2\mu\text{m}$  device (b) resonance at 4.15 KHz

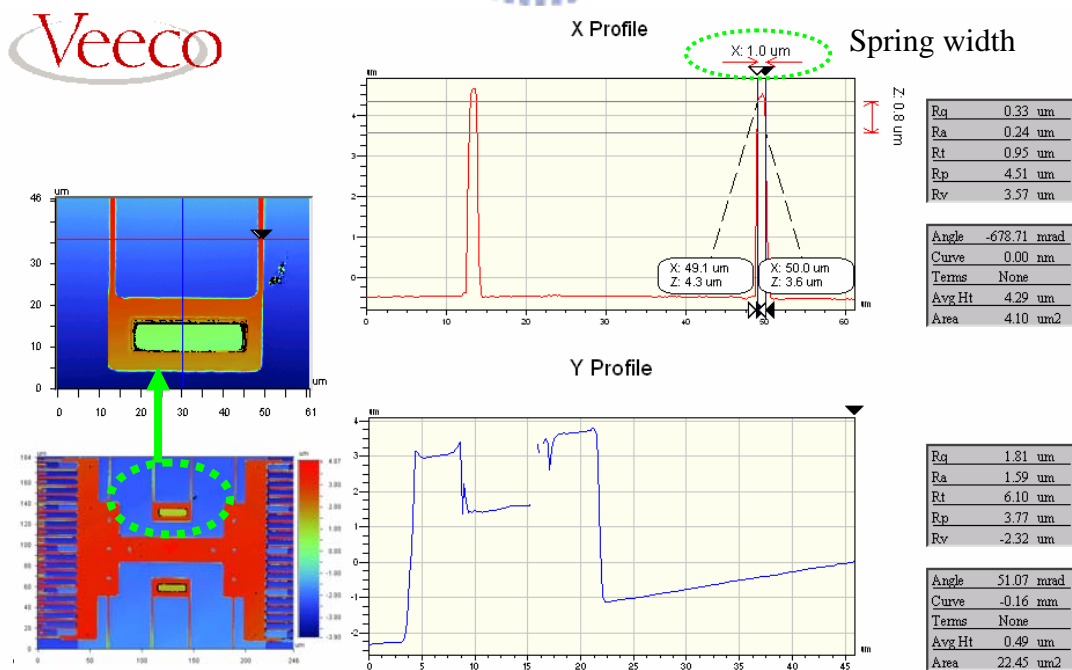


Fig 4-7 Spring width of  $2\mu\text{m}$  device by WYKO measurement

## 4-2 Optical spot size measurement by MUMPs devices

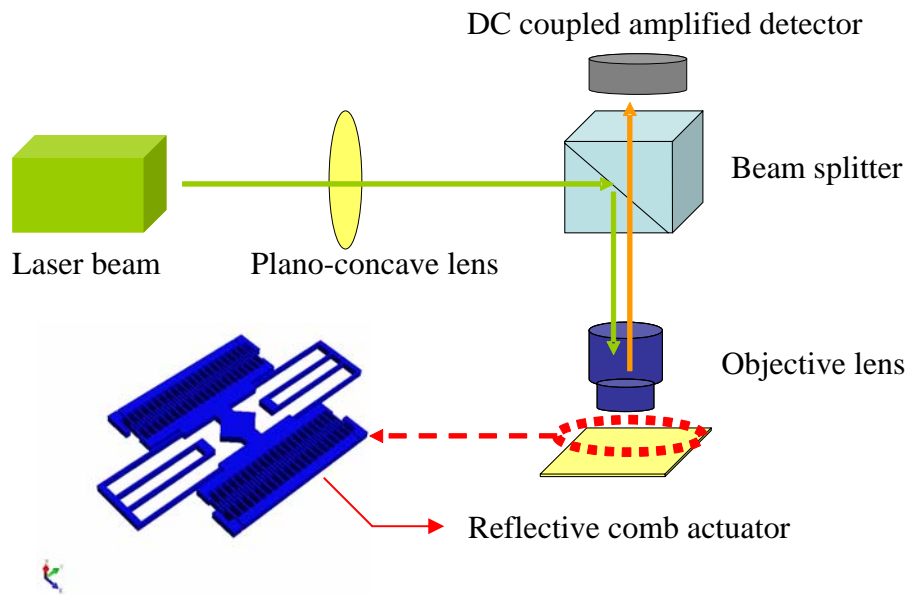
The setup for the reflection type spot scan system is shown Fig 4-8. A DC coupled amplified photo detector THORLABS PDA 155 is used to detect the signal from the reflective knife-edge plate. The specification of the photo detector is listed in Table 4-2 and its spectral responsivity is shown in Fig 4-9.

In the optical path, a plano-concave lens is used to expand the laser beam before entering the focusing objective lens. The FWHM of the laser beam after the beamsplitter is measured to be around 20mm, which is sufficiently large to fill the apertures of typical 20X and 40X objectives. The powers of the laser sources are 0.8mW for the green (543nm) He-Ne laser and 5mW for the red (633nm) He-Ne laser.

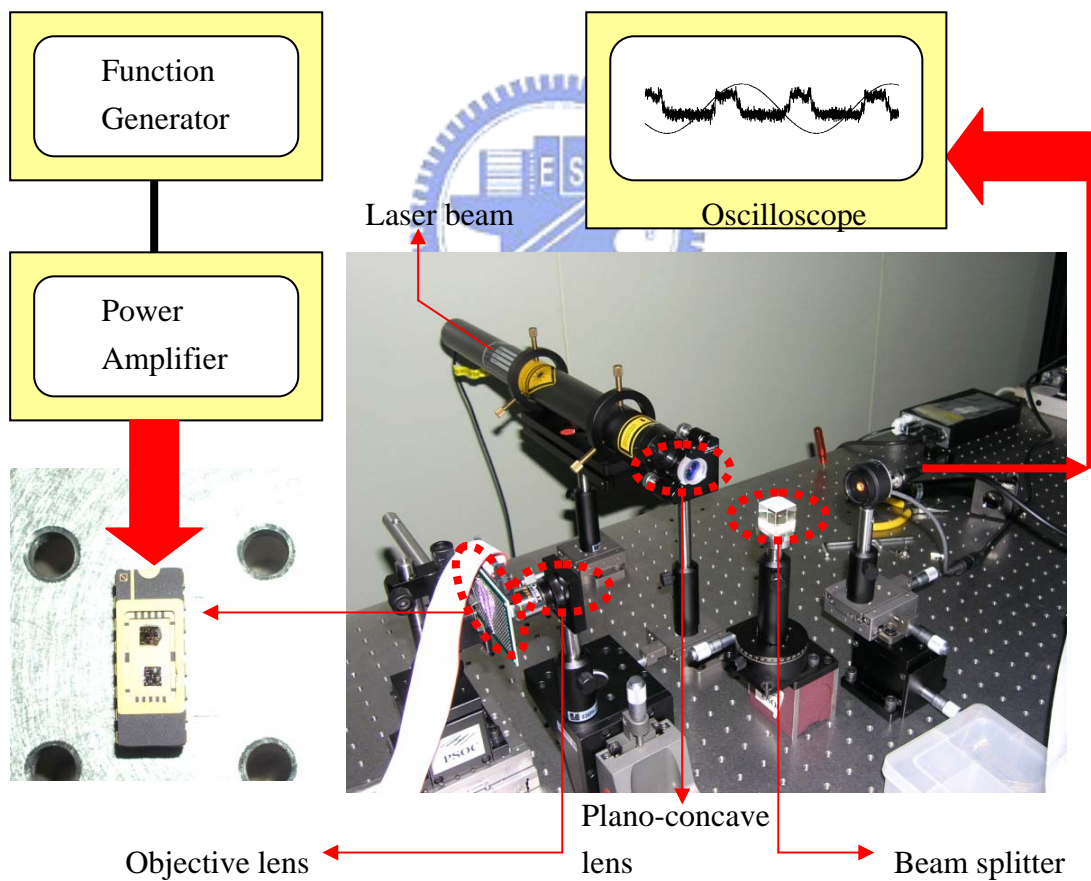
When the knife-edge plate is driven to vibrate periodically, the observed waveform of the photocurrent can be shown schematically in Fig 4-10. If the vibration amplitude of the knife-edge plate is larger than twice the diameter of the optical spot, the spot can be scanned in two orthogonal directions in one half of the scan cycle. Therefore, the spot is scanned four times in one full scan cycle, as shown in Fig 4-10(a). The spot profile along the two orthogonal directions can be derived from the measured photocurrent using Eq 1-2, as shown in Fig 4-10(b).

If the triangular reflective area does not fully cover the scanning plate, light can be reflected from the surrounding polysilicon region and distorted the measured signal. Even though the distortion may be small due to the large difference between the reflectivity of the metal layer and the polysilicon structure, this effect certainly needs to be considered in high accuracy measurement.





(a)



(b)

Fig 4-8 (a) Schematic, (b) setup of the reflection type spot size measurement



Detector	Silicon
Active Area	0.8mm <sup>2</sup> (Ø1.0mm)
Response	200 to 1100 nm
Peak Response (typ)	0.45 A/W (750nm)
Small Signal Bandwidth <sup>1</sup>	50MHz (min.)
NEP (960 nm)	4 x 10 <sup>-11</sup> W/√Hz (max.)
Noise (RMS)	2.0mV (max.)
Dark Offset	20mV (max.)
Output Voltage (50Ω)	0 to 5V
Output voltage	0 to 10V
Transimpedance Gain	1 x 10 <sup>4</sup> V/A (5 x 10 <sup>3</sup> V/A with a 50Ω terminator)

Table 4-2 Specification of photo detector PDA 155 by THORLABS

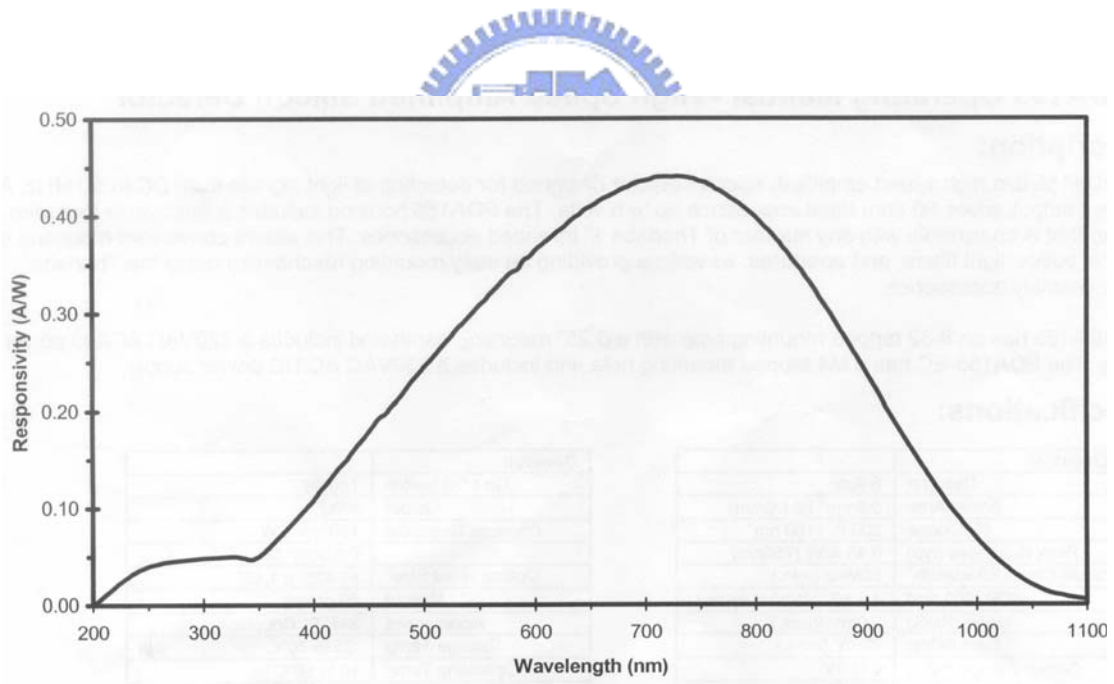
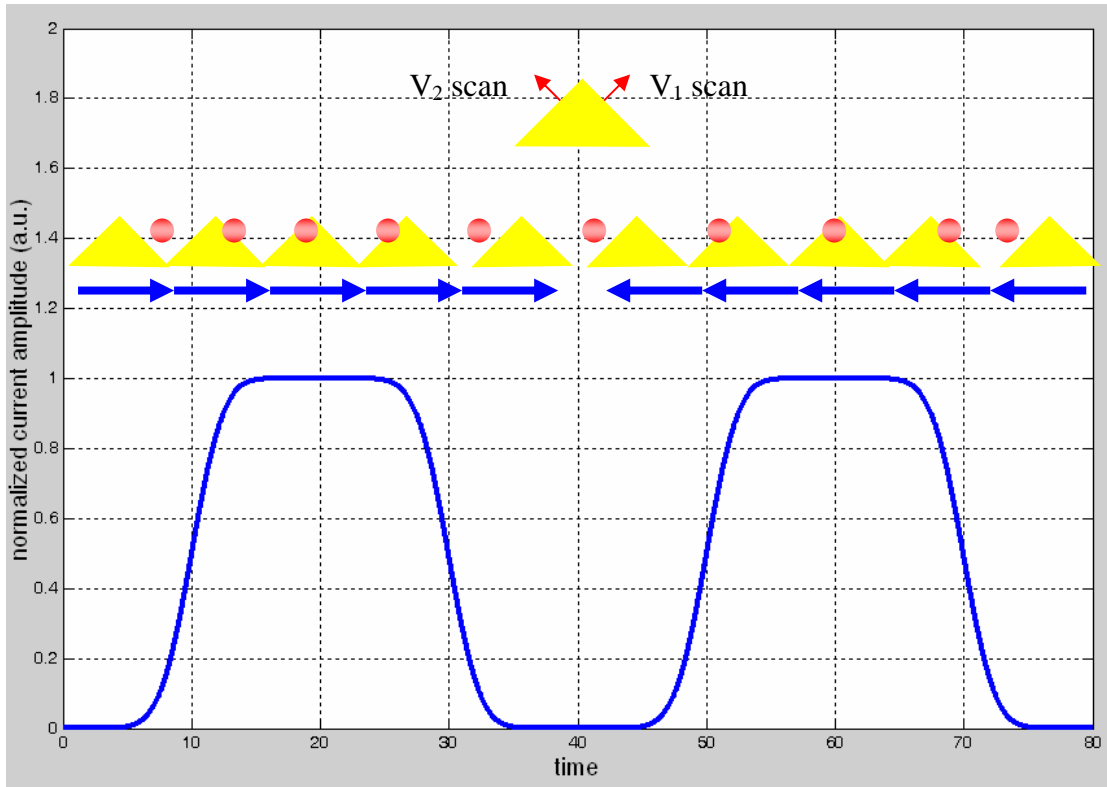
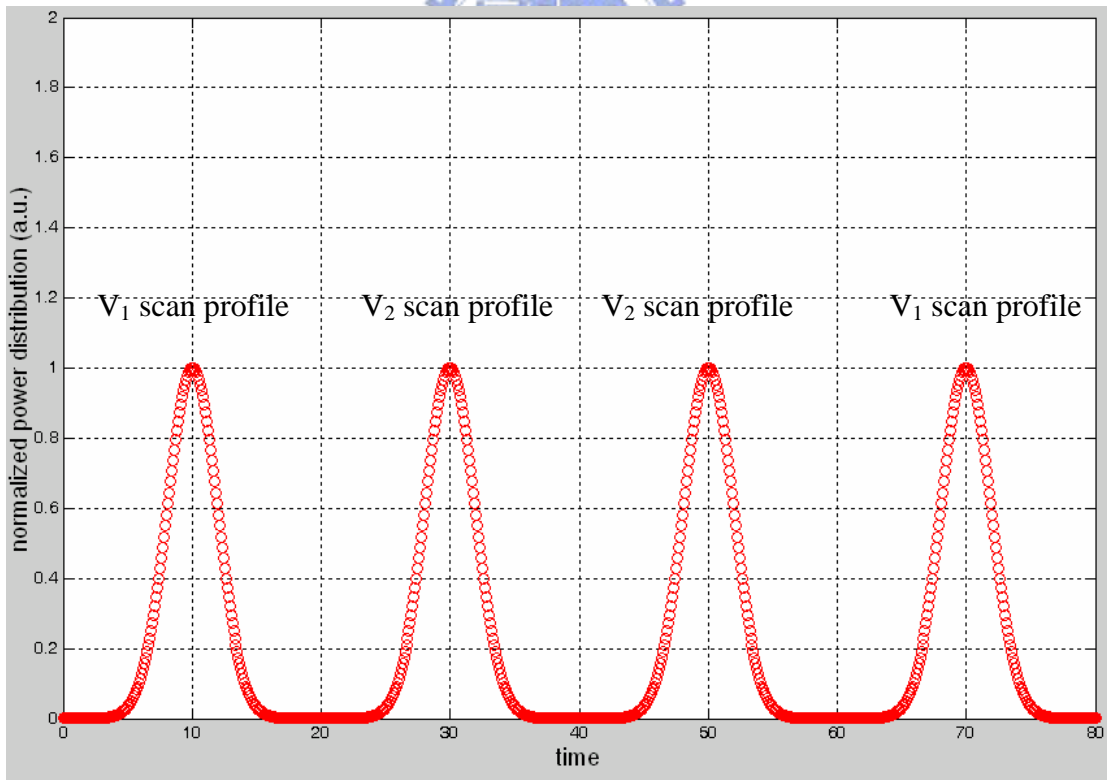


Fig 4-9 Spectral responsivity curve of PDA 155



(a)



(b)

Fig 4-10 (a) Observed waveform of photocurrent in an oscilloscope for a full scan cycle, (b) beam profile derived from the photocurrent measurement

When a periodic driving voltage was applied to the actuator to vibrate at its resonance frequency, the observed signals for two different light sources are shown in Figs. 4-11 and 4-12. The sinusoidal wave is the signal applied to the comb actuator from function generator and all of the waves are shown in the time domain. The irregular peaks in the photocurrent waveform are due to the laser noise, the interference of the optical path, roughness of reflective mirror and electrical noise of photo detector.

To derive the spot profile from the photocurrent waveform, the knowledge of the relation between the position of knife-edge plate and the driven voltage is needed. Assume the applied voltage is:

$$V(t) = V_{DC} + V_{AC} \sin(2\pi f_0 t) \quad (4-1)$$

where  $f_0$  is the resonance frequency. The static displacement of a comb actuator is proportional to  $V^2(t)$ .

$$\begin{aligned} V^2(t) &= (V_{DC} + V_{AC} \sin(\omega_n t))^2 \\ &= \left(V_{DC}^2 + \frac{V_{AC}^2}{2}\right) + 2V_{DC} V_{AC} \sin(2\pi f_0 t) - \frac{V_{AC}^2 \cos(2 \times 2\pi f_0 t)}{2} \end{aligned} \quad (4-2)$$

Therefore, there is a second harmonic component in the driving voltage. However, the displacement response at this high frequency is very small compared to the peak resonance displacement in a high-Q resonance system. Therefore the plate can be assumed to vibrate exactly at the resonance frequency only. Further more, there is a  $90^\circ$  phase shift between the input driving voltage and the output plate displacement in a second order system at resonance. As a result, for a sine wave driving voltage, the position of the scanning plate is proportional to a cosine wave, i.e.  $x(t) \propto \cos(2\pi f_0 t)$ .

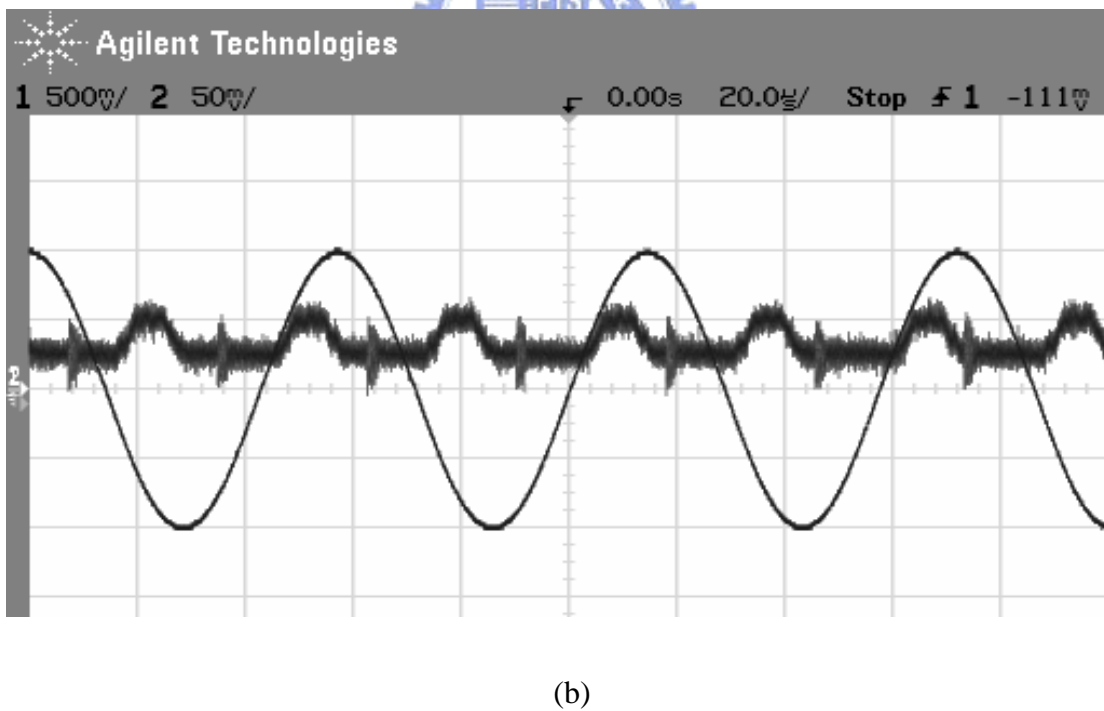
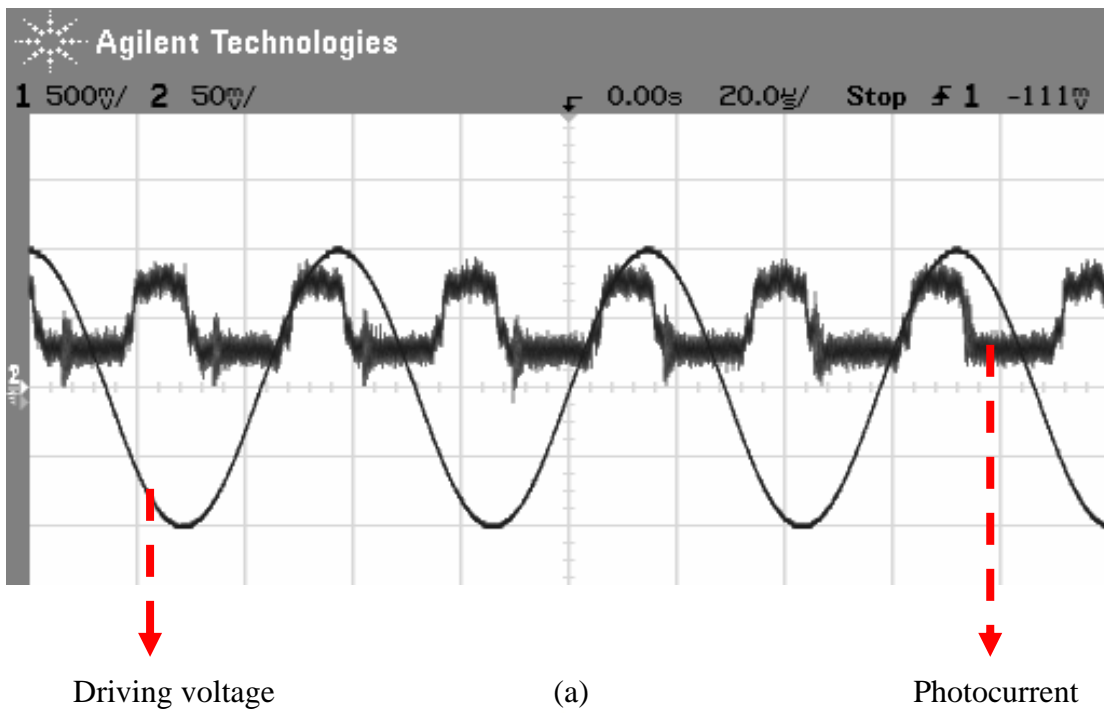


Fig 4-11 Observed signals of spots focused with a (a) 20X and (b) 40X objective lens for green (543nm) light

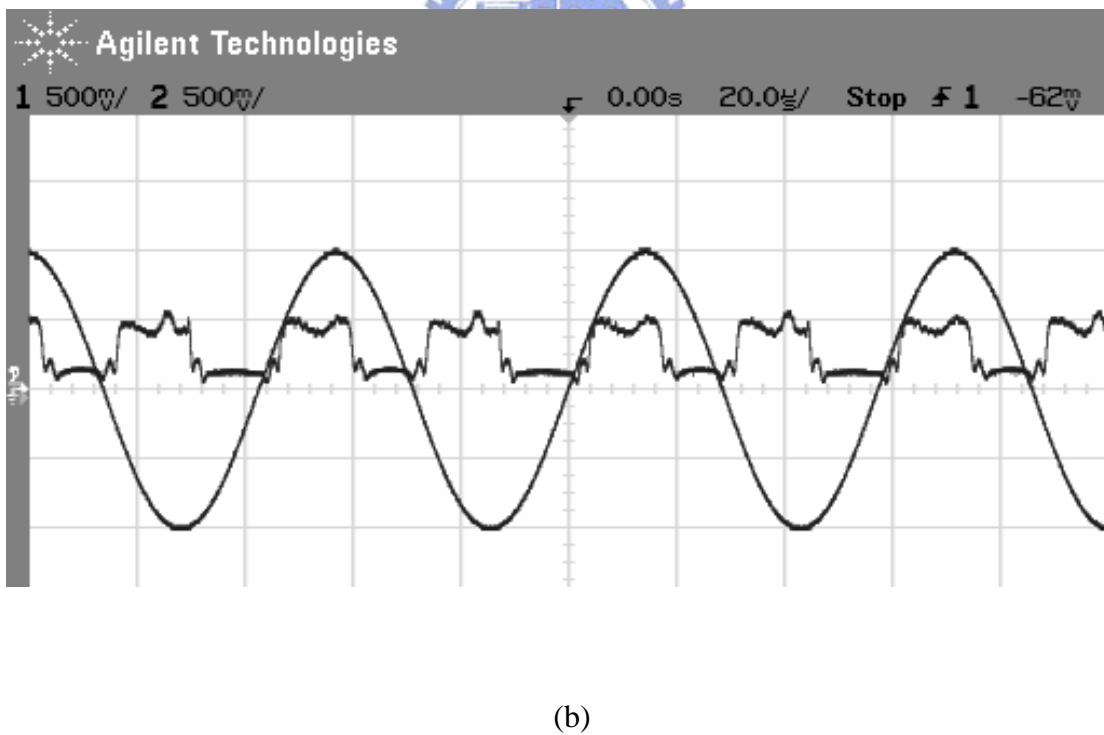
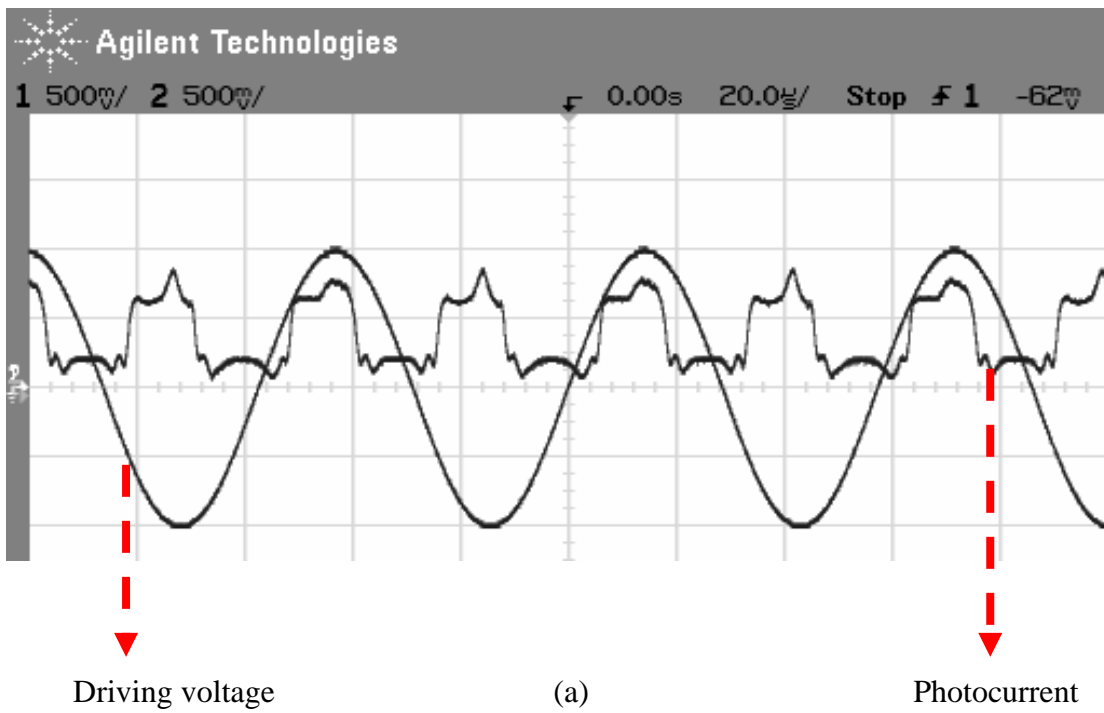
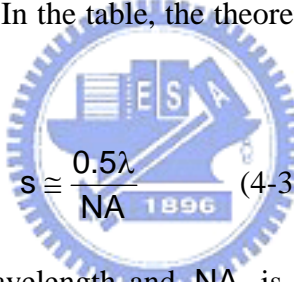


Fig 4-12 Observed signals of spots focused with a (a) 20X and (b) 40X objective lens for red (633nm) light

Figs 4-13 and 4-14 show the acquired photocurrent data in Figs 4-11 and 4-12, respectively, plotted vs. a cosine function. All the actuators are driven with  $V_{DC} = 80V$  and  $V_{AC} = 160V$ . The two orthogonal scanning can be seen clearly. A running average filter with 11 points is used to reduce the measurement noise, as the solid lines indicate. Note that the number of points should not be too large in order not to affect the edge transition width of the measured waveform. As shown in Fig 4-13,  $D$  is the amplitude of resonance,  $I_{max}$  and  $I_{min}$  are the maximum and minimum values of the photocurrent, respectively,  $\Delta I$  is the difference of  $I_{max}$  and  $I_{min}$ , and  $W_1$  and  $W_2$  are the positions corresponding to  $I_{min} + 0.12\Delta I$  and  $I_{max} - 0.12\Delta I$ .

The FWHM of the optical spot can be calculated from  $W_2 - W_1$ . The calculated results are listed in Table 4-3. In the table, the theoretical minimum FWHM spot size  $s$  are calculated by [26]:



$$s \cong \frac{0.5\lambda}{NA} \quad (4-3)$$

where  $\lambda$  is incident laser wavelength and  $NA$  is the numerical aperture. For the 20X and 40X objectives, the  $NA$  are 0.4 and 0.65, respectively.

Table 4-3 Measured and theoretical spot size

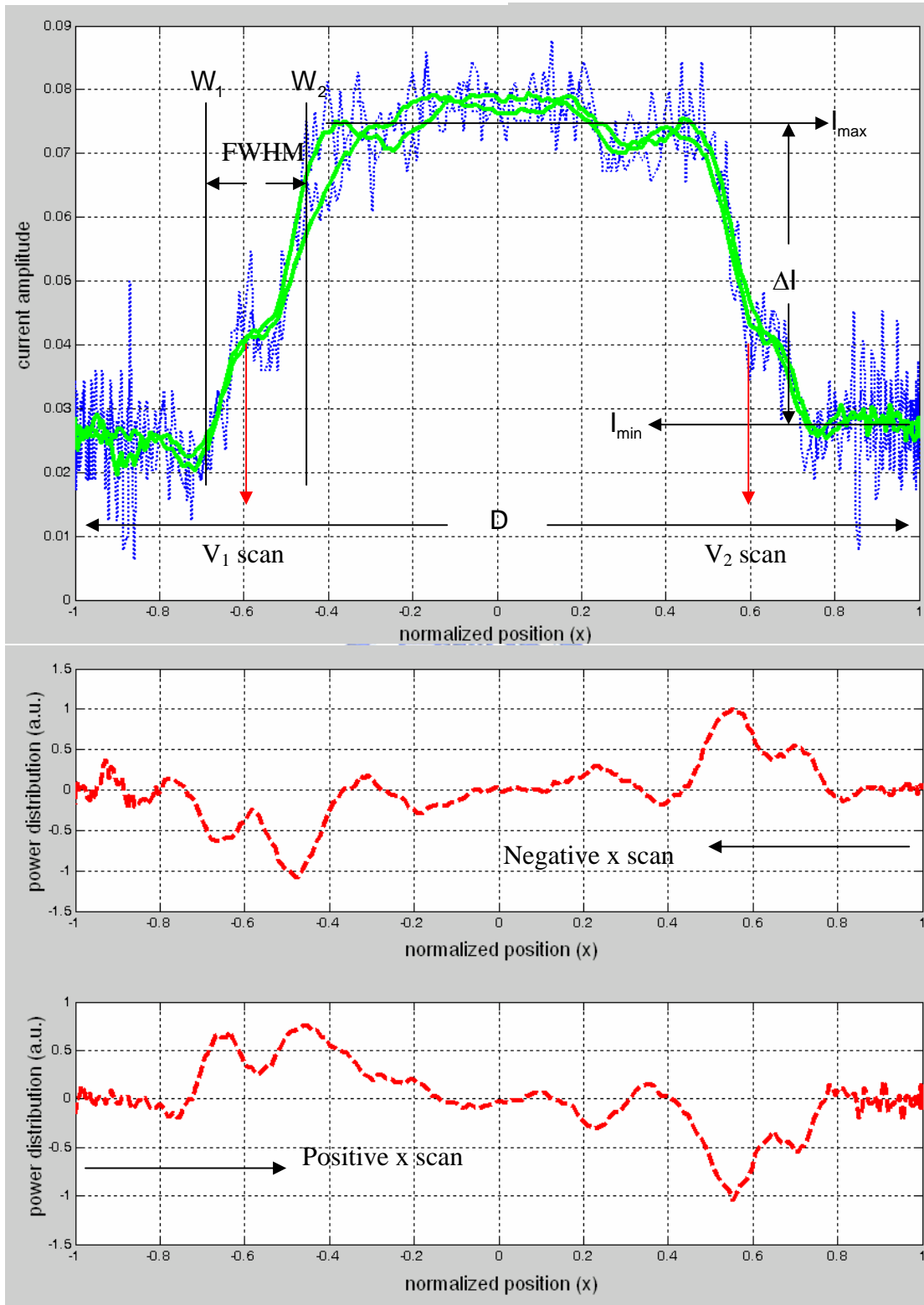
	$I_{max}$	$I_{min}$	$D(\mu m)$	Spot size ( $\mu m$ )	
				Measured	Theoretical minimum
20X,543nm,0.8mW	0.074	0.025	20	2.7	0.68
40X,543nm,0.8mW	0.055	0.025	20	1.9	0.44
20X,633nm,5mW	0.65	0.25	20	0.8	0.79
40X,633nm,5mW	0.45	0.12	20	1.75	0.53

In general, the preliminary results show spot sizes much larger than the theoretical min spot size. This is due to the non-optimized optical focusing system, non-ideal laser output profile, laser noise, and electrical noise due to small reflected optical signal.



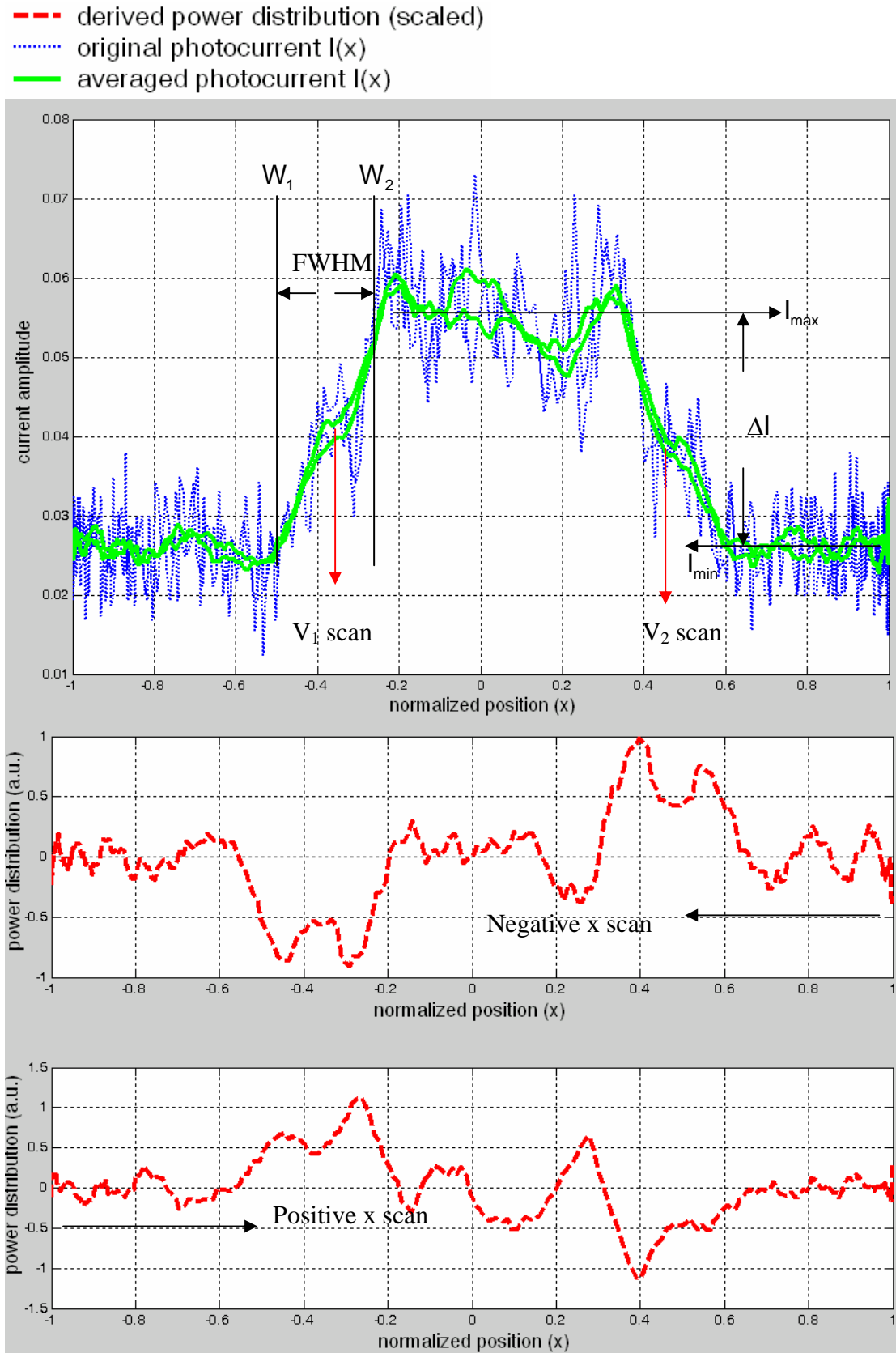


- derived power distribution (scaled)
- ... original photocurrent  $I(x)$
- averaged photocurrent  $I(x)$



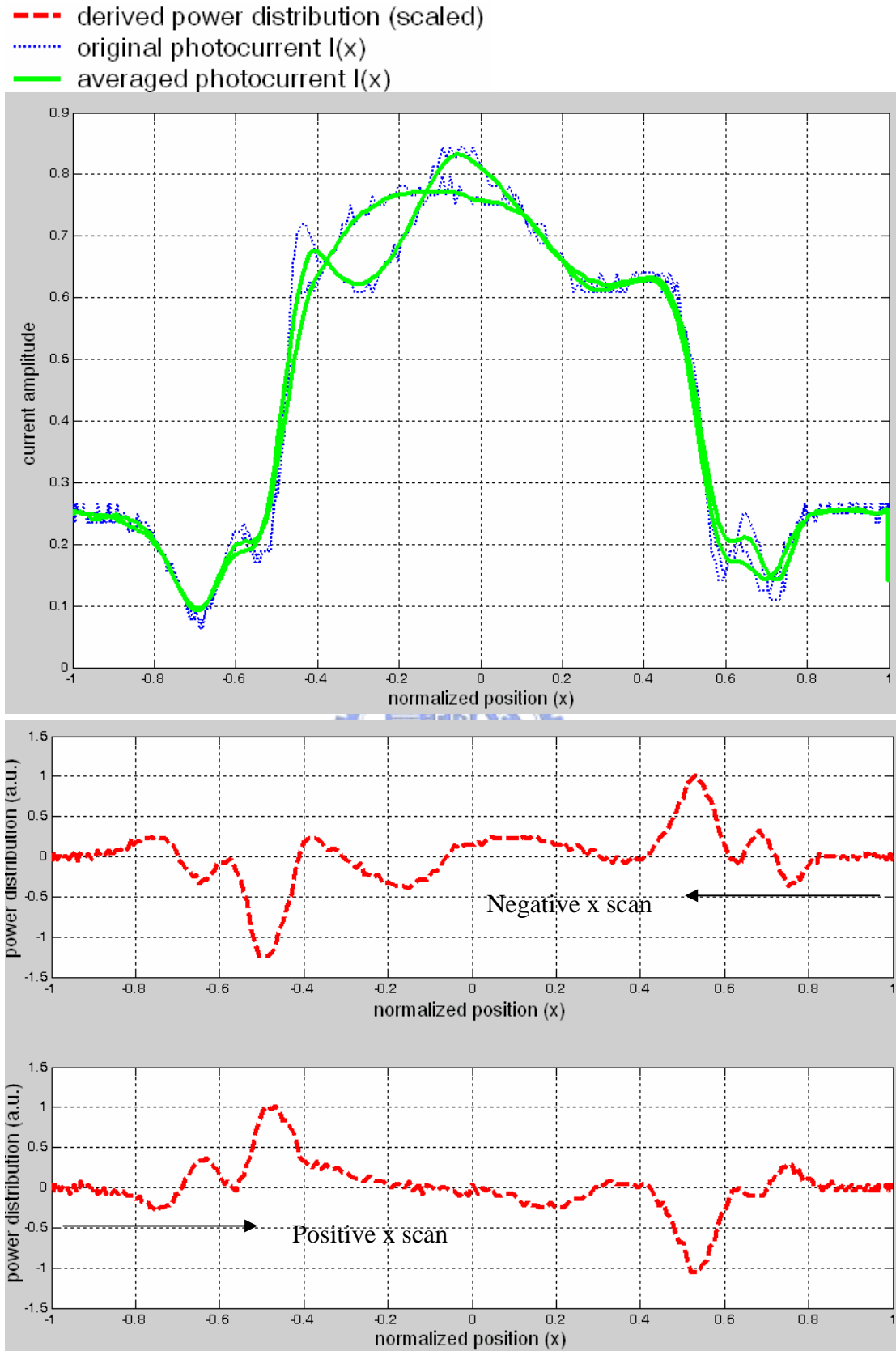
(a)

Fig 4-13 Measured photocurrent and derived power distribution of the spot with (a) 20X and (b) 40X objective lens for the green (543nm) light



(b)

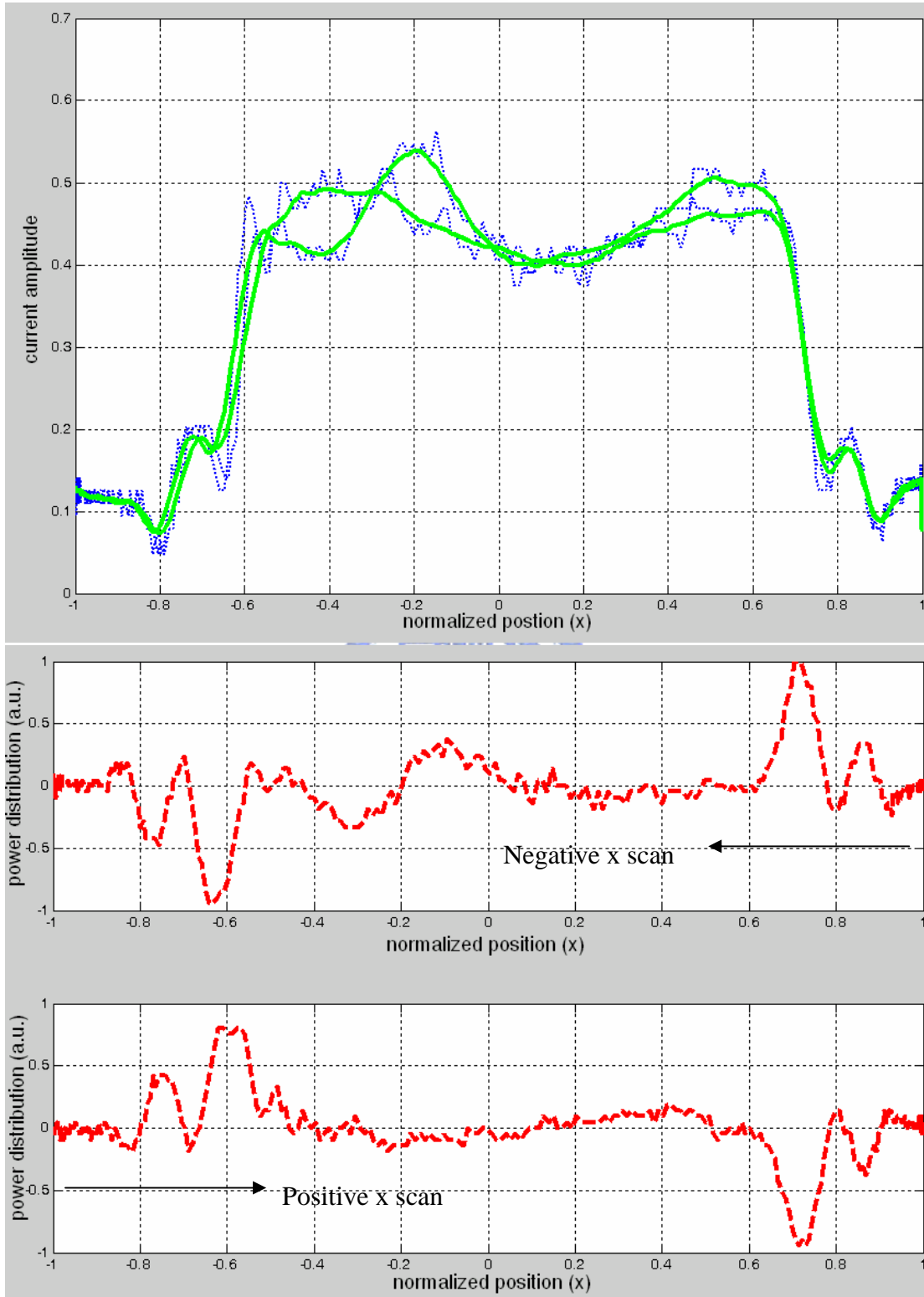
Fig 4-13 Measured photocurrent and derived power distribution of the spot with (a) 20X and (b) 40X objective lens for the green (543nm) light (continued)



(a)

Fig 4-14 Measured photocurrent and derived power distribution of the spot with (a) 20X and (b) 40X objective lens for the red (633nm) light

- derived power distribution (scaled)
- ... original photocurrent  $I(x)$
- averaged photocurrent  $I(x)$



(b)

Fig 4-14 Measured photocurrent and derived power distribution of the spot with (a) 20X and (b) 40X objective lens for the red (633nm) light (continued)

### 4-3 Responsivity of photo detector

The setup of the photo detector responsivity measurement consists of a semiconductor characterization system and a light source, as shown in Fig 4-15. The light source is a 0.8mW He-Ne laser at 543nm wavelength. The laser beam diameter (0.8mm) is the width at  $1/e$  (36.8%) of power density. The I-V curves of the photo detector are measured by a Keithley 4200-SCS semiconductor characterization system. The measured sample is from the first run of the  $\langle 111 \rangle$  silicon substrate fabrication. The photo detector layout used in the measurement is shown in Fig 4-16(a). From a WYKO measurement, the area of the triangular photo detector is about  $3.24 \times 10^{-4} \text{ cm}^2$ , as shown in Fig 4-16(b).

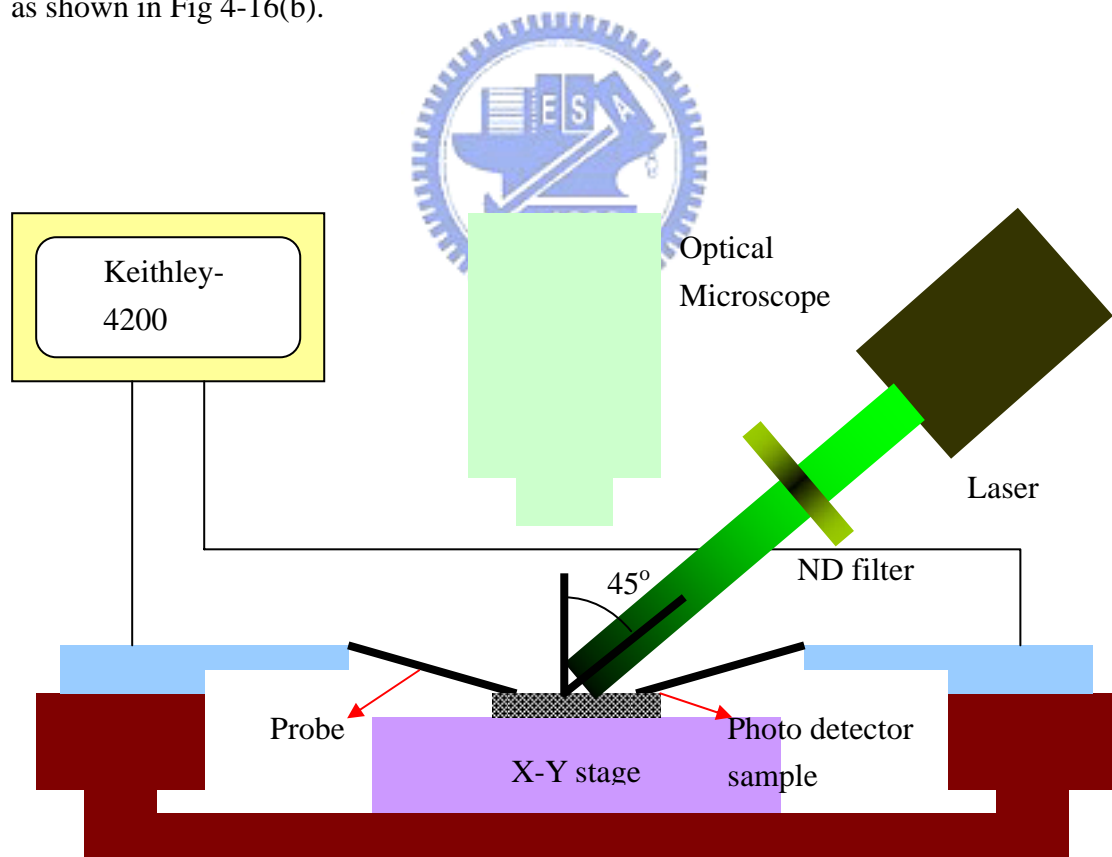
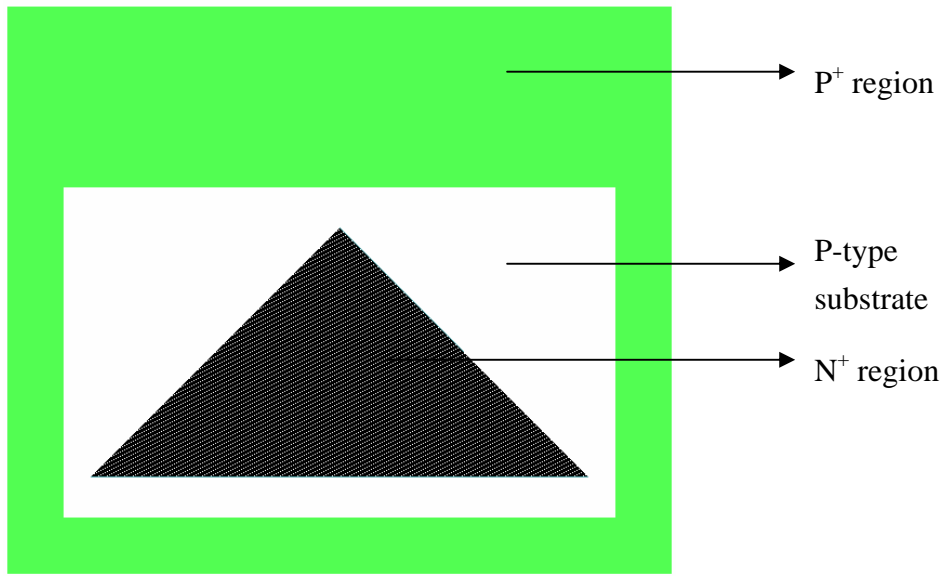
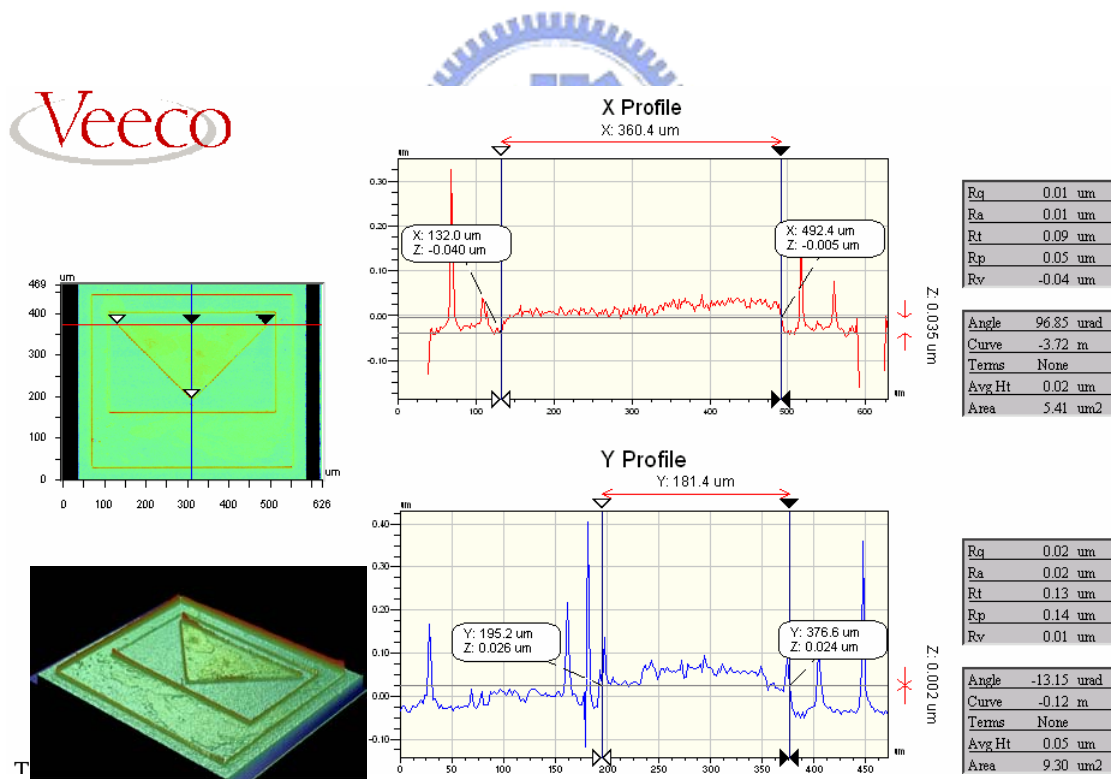


Fig 4-15 Experimental setup for I-V curve measurement



(a)



(b)

Fig 4-16 (a) Photo detector layout (b) area of the photo detector measured by the WYKO interferometer

If the 0.8mW laser beam is assumed to have a Gaussian profile with a 1/e radius of  $0.8/2=0.4\text{mm}$ , the power density profile can be written as [26]:

$$P_i = 0.23 \times e^{-6.25r^2} \text{ W/cm}^2 \quad (4-4),$$

where  $r$  is the radial distance (in cm) from the center of the spot. Since the incident light is tilted at  $45^\circ$  with respect to the detector surfaces, the incident power density becomes:

$$P_0 = 0.23 \times e^{-6.25r^2} \times \cos 45^\circ = 163e^{-6.25r^2} \text{ mW/cm}^2 \quad (4-5)$$

Different incident power levels were generated by placing an ND filter with optical density (OD) of 1 and 2 in front of the laser. The ND filter with an OD value of 1 attenuates the power of light by a factor of 10. The incident powers  $P_1$  and  $P_2$  with ND filters with OD values 1 and 2, respectively,

$$P_1 = 0.1 \times 0.23 \times e^{-6.25r^2} \times \cos 45^\circ = 16.3e^{-6.25r^2} \text{ mW/cm}^2 \quad (4-6)$$

$$P_2 = 0.01 \times 0.23 \times e^{-6.25r^2} \times \cos 45^\circ = 1.63e^{-6.25r^2} \text{ mW/cm}^2 \quad (4-7)$$

The measured I-V characteristics by Keithley 4200 for different incident laser power levels are as shown in Fig 4-17. Relatively constant photocurrent is observed with increasing reverse bias voltage. The dark current is measured to be less than 15nA for the applied voltage ranged from 0V to 15V. If the photo detector is assumed to be  $r = 0$ , the responsivity of the  $5 \times 10^{-3} \text{ cm}^2$  photo detector at incident laser powers of  $163 \text{ mW/cm}^2$ ,  $16.3 \text{ mW/cm}^2$  and  $1.63 \text{ mW/cm}^2$  are plot in Fig 4-18 and compared to the calculation in Fig 2-13. The difference between measurement and calculation is mainly attributed to the minority carrier lifetime, the actual laser power distribution, and the actual position of the detector. The mismatch of the two responsivity curves at laser power =  $163 \text{ mW/cm}^2$  and  $16.3 \text{ mW/cm}^2$  can be attributed



to the shift of optical spot of interference during measurement. The irregular characteristics of the responsivity at laser power =  $1.63 \text{ mW/cm}^2$  results from the insufficient incident power density and low output signal.

#### **4-4 Summary**

The resonance magnitude and frequency of the comb actuator of the reflection type spot system fabricated using MUMPs technology were measured. Mismatch between the theoretical and measured values due to the fabrication tolerance was discussed and corrected.

The reflection type scan system was used to measure the spot size. The preliminary results showed larger spots compared to the diffraction limit due to non-ideal measurement set up.

Finally, the responsivity of photo detectors in the absorption type device was measured and showed relatively good agreement with the calculation value.

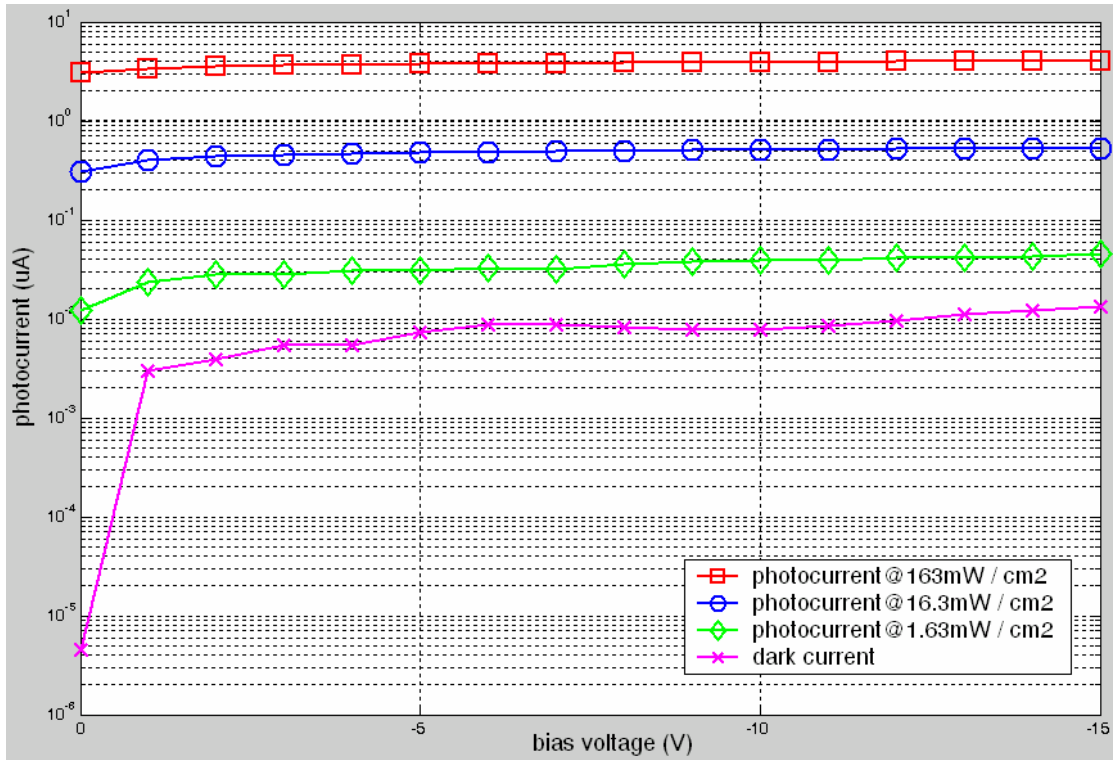


Fig 4-17 Measured I – V characteristics of the photo detector

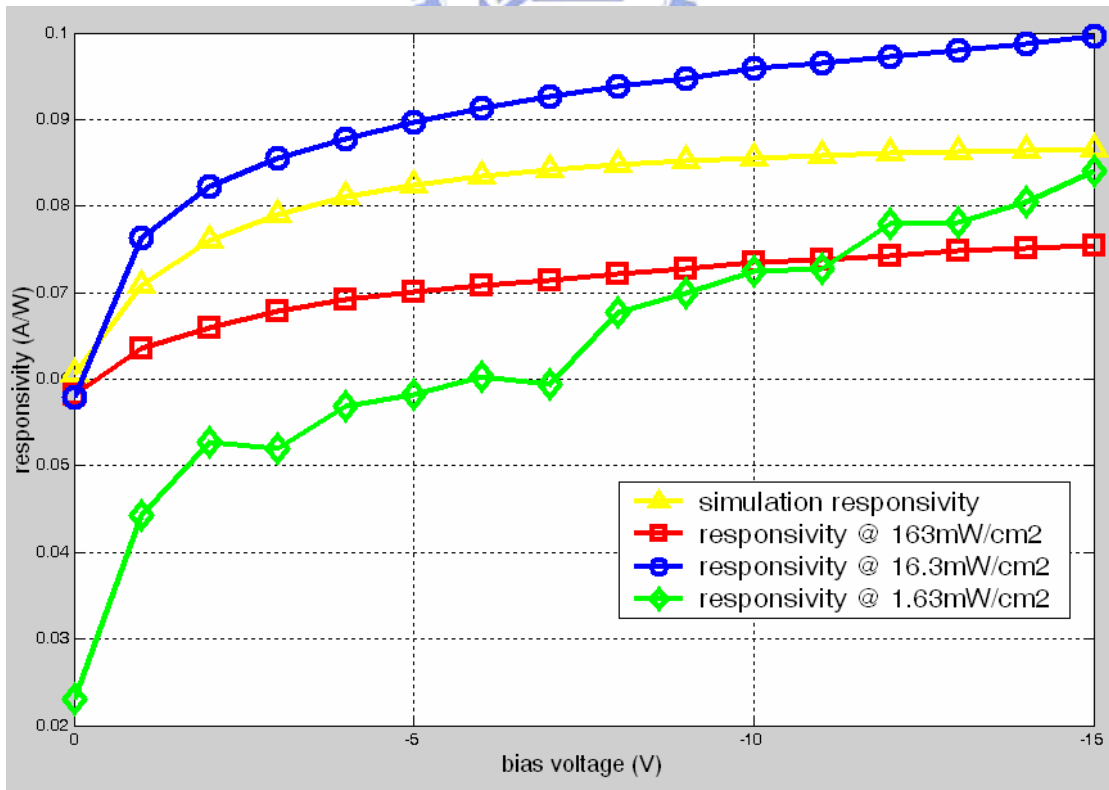


Fig 4-18 Measured responsivity and simulation characteristics of photo detector